Microstructures and Magnetic Properties of Heatproof Domain-Refined Grain-Oriented Silicon Steel Sheets

K. Kosuge, K. Hirose, and K. Kuroki

Microstructures and magnetic properties of heatproof domain-refined grain-oriented silicon steel sheets were studied. Local strains were introduced using two types of gear roll as well as cog tips, one 35 μm and the other 85 μm. After the local strains were introduced onto sheets, the distribution of hardness near the groove was measured. The nuclei of micrograins were investigated at various applied rolling loads. After stress-relief annealing, various shapes of micrograins and grooves were observed. The effect of these various shapes of grooves and micrograins on magnetic properties was clarified. The role of micrograins and grooves on domain refining is discussed.

Keywords
domain-refined, grain-oriented, groove, micrograin, silicon steel sheets

1. Introduction

IT is very important to reduce the core loss of grain-oriented electrical steel sheets. Various attempts to reduce iron loss have been made, such as improving orientation, using thinner gage, having small grain size after secondary recrystallization, tensile stress coating, and domain refining.

Domain refinement is one of the most effective techniques for reduction of core loss of grain-oriented electrical steel sheet with high permeability (HI-B) (Ref 1, 2). Nippon Steel Corporation developed the laser scribing method (Ref 3-5). The resultant product marketed under the name of 'ZDKH.' This method is very useful in electrical steel sheets for stacked core transformers, but the effect of domain refining is diminished after stress-relief annealing (SRA), which is necessary in the manufacturing of wound-core transformers in order to relieve the stress induced during the winding process. For this reason, the heatproof, domain-refined material for wound-core transformers is in demand.

Several methods for making heatproof, domain-refined materials have been researched. Nippon Steel Corporation recently presented three methods for development: the chemical etch pit method (Ref 6), the Sb doping method (Ref 7), and the local strain introduction and heat treatment method (Ref 8). The resultant product using the combination of local strain and a heat treatment was marketed under the name 'ZDMH.' The effect of various shapes of grooves and micrograins on magnetic properties was not clarified (Ref 7, 9).

Experimental results of the practical heatproof domain-refining technique using the combination of a local strain and a heat treatment, which is applied to the final texture annealed materials, are presented in this paper. The mechanism of growth of micrograins is made clear, and the effect of various shapes of grooves and micrograins on magnetic properties is clarified. From the previous domain patterns observed with a high voltage scanning electron microscope (SEM) (Ref 7), the role of grooves and micrograins on magnetic properties is clarified. Magnetostatic energy of grooves and micrograins is discussed.

K. Kosuge and **K. Hirose,** Hirohata R&D Laboratories, Nippon Steel Corp., and **K. Kuroki,** Yawata R&D Laboratories, Nippon Steel Corp., 1, Fuji-Cho, Hirohata-ku, Himeji-City Hyogo, Japan

2. Experimental Procedure

Samples consist of 30-mm-wide, high-permeability, grain-oriented 3% Si-Fe(HI-B) sheet of 11 mil (0.27 mm) thickness with glass film.

Local strains were introduced by a gear-type roll under an applied load of 59 to 118 kg for 30 mm-wide sheets, in which 10 to 40 μm deep grooves were made. This process used two types of gear roll as well as cog tips, one 35 μm and the other 85 μm. Each shape of the cog tip was flat. Then the steel sheets were subjected to heat treatment at 850 °C for 4 h (SRA). In this way, various shapes of micrograins and grooves were generated in the sheets. The groove lines on the steel sheet were declined to 75° toward the rolling direction. The pitch of the groove was 5 mm. As shown in Fig. 1, the apparatus consisted of the gear (strain-introduced roll) and a press roll, which was forced upwards using the back-up rolls. The gear roll was provided opposite to a press roll, which was pressed upwards by four back-up rolls arranged in a longitudinal direction. The gear roll was 100 mm long and 110 mm in diam. The press roll was 80 mm in diam. Each pair of back-up rolls was pressed upwards by a hydraulic cylinder, which was used so that each respective back-up roll pressed against the press roll with the same oil pressure.

The distribution of hardness (HV 25 g load) near the groove was measured after the local strains were introduced onto sheets. The nuclei of micrograins were investigated at various conditions with an applied load of 59 to 118 kg and annealed at 600 to 900 °C for 0 to 30 min. After SRA, various shapes of micrograins and grooves were observed.

Magnetic properties of these samples before and after domain refinement were measured using a single sheet tester.

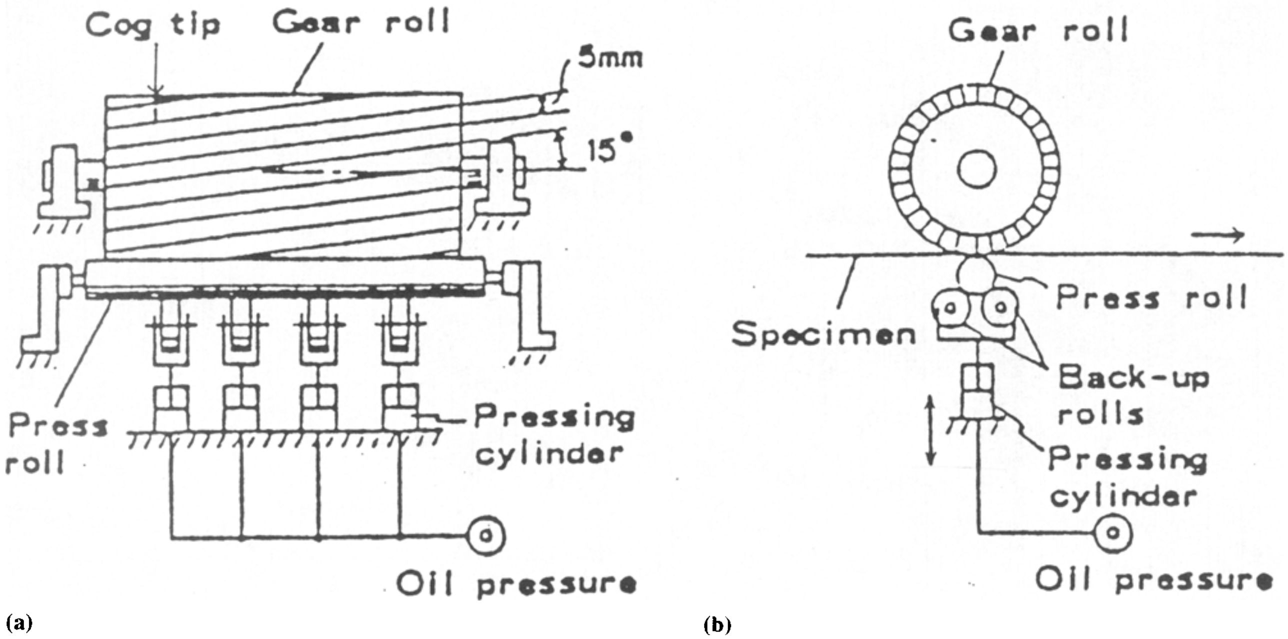

Fig. 1 Apparatus for strain introduction. (a) Front view. (b) Side view

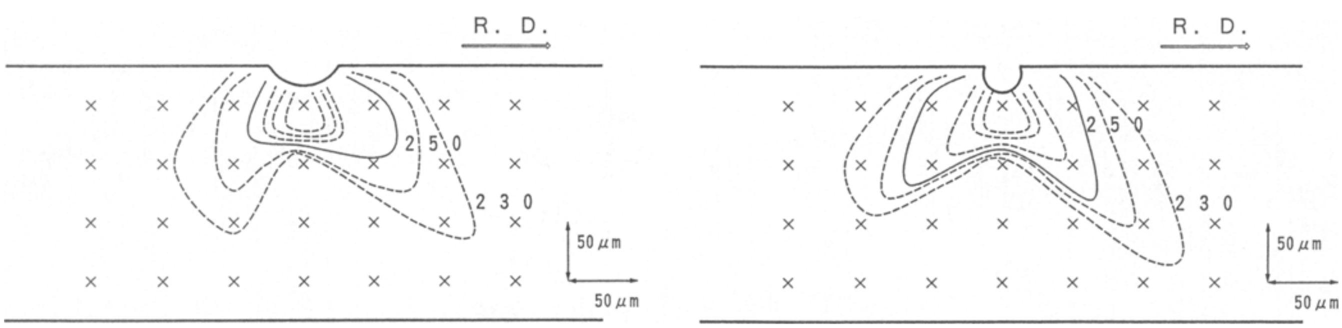

Fig. 2 Distribution of hardness after rolling. Total load is 88 kg. (a) width of a cog tip was 85 μm. (b) width of a cog tip was 35 μm.

3. Results and Discussion

3.1 *Nucleus of Micrograins*

Figure 2 shows the distribution of hardness after the local strains were introduced onto sheets. Total gear load was 88 kg. Width of a cog tip was 85 μm (Fig. 2a) and 35 μm (Fig. 2b). Distribution of the 85 μm tip was broader than that of the 35 μm tip. The portion with the highest level of hardness was distributed at 45° angles from the surface of the sheet. The 35 μm tip was sharper and deeper on the sheets compared to the 85 μm tip. Distribution was the same as ball-point scratching (Ref 10).

Figure 3 shows the nucleus of micrograins annealed at 700 °C for one-half hour on the 85 μm tip. Total load was 74 kg. The micrograins were generated from the surface of grooves and grew in 45° angles, which is the same direction as for the distribution of the highest level of hardness. Recovery can be observed in the same area.

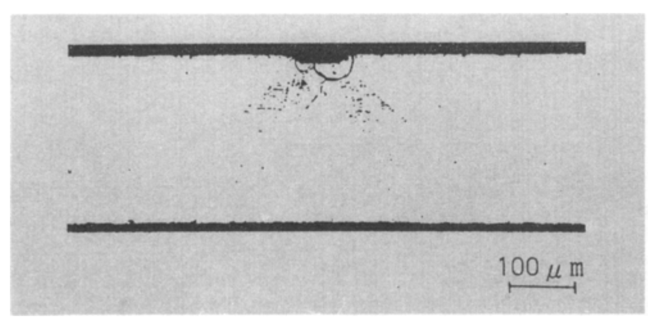

Fig. 3 Nucleus of micrograins (total load 74 kg, the 85 μm tip). Annealed 700 °C for 30 min

3.2 *Texture at Strain-Introduced Site*

Figure 4 shows the cross-sectional views of texture at the sites of various strain introductions followed by SRA. As the

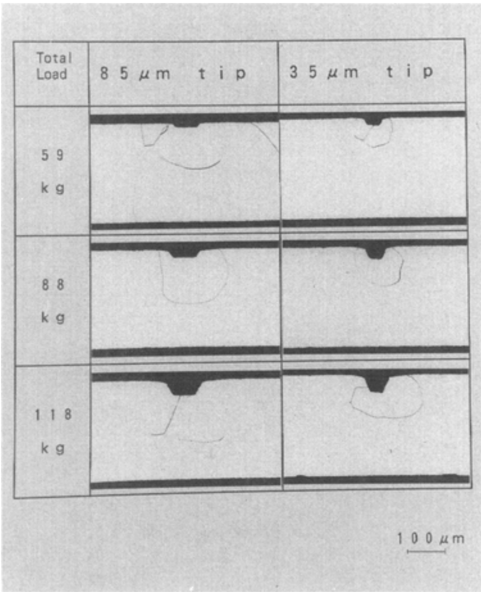

Fig. 4 Cross-sectional views of texture at the sites of various introductions, followed by SRA

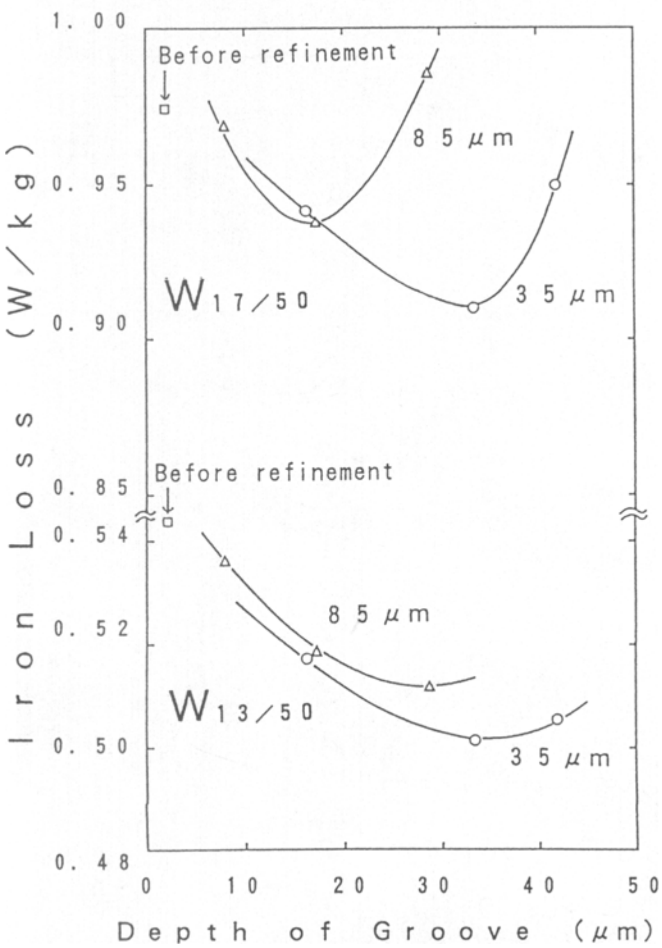

Fig. 5 Relationship between the depth of grooves formed on a steel sheet and their magnetic properties

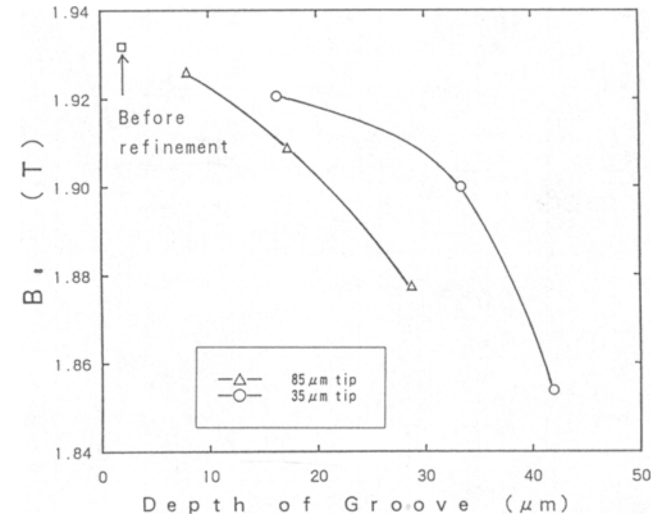

Fig. 6 Relationship between the depth of grooves formed on a steel sheet and their magnetization

rolling load increased, the depth of grooves and micrograins increased. In the case of the 85 μm tip, the groove had a shallow and wide shape. The shapes of micrograins were deep and wide. On the other hand, in the case of the 35 μm tips, the groove had deep and narrow shapes. The shapes of micrograins were circular and smaller when compared with the 85 μm tip. Regarding the distribution of the highest level of hardness, the micrograins of the 85 μm tip would be recovered at a broad place and grow larger.

3.3 *Groove Shapes Versus Magnetic Properties*

Magnetic properties of these various types of domain-refined sheets were measured.

Figure 5 shows the relationship between the depth of grooves formed on a steel sheet and their magnetic properties. In each width of the tip, the optimum depth of grooves was different. In the case of the 85 μm tip, the iron loss of $W_{17/50}$ was a minimum at 15-μm-deep grooves, and of $W_{13/50}$, at 30-μm-deep grooves. On the other hand, the 35 μm tip had a minimum iron loss of $W_{17/50}$, at 40-μm-deep grooves, and of $W_{13/50}$, at 35-μm-deep grooves. The effect of decreasing iron loss is larger in the 35 μm tip than in the 85 μm tip.

Figure 6 shows the relationship between the depth of grooves formed on a steel sheet and their magnetization B_8. In both widths of tips, as the depth of groove increased, the magnetization B_8 decreased because the micrograin would affect the decreasing of the magnetization B_8. The effect of decreasing induction B_8 via the depth of grooves was larger in the 85 μm tip than in the 35 μm tip. If a groove and micrograins were present in the sheet, the magnetic flux would not be horizontal. The 35 μm tip with small micrograins had a small effect on the magnetization compared to the 85 μm tip with large micrograins.

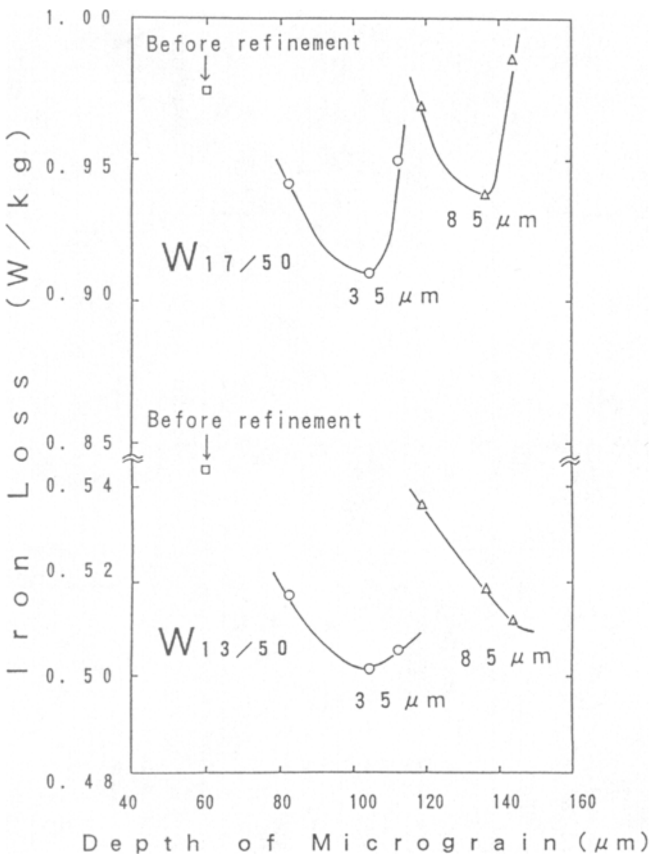

Fig. 7 Relationship between the depth of micrograins formed on a steel sheet and their magnetic properties

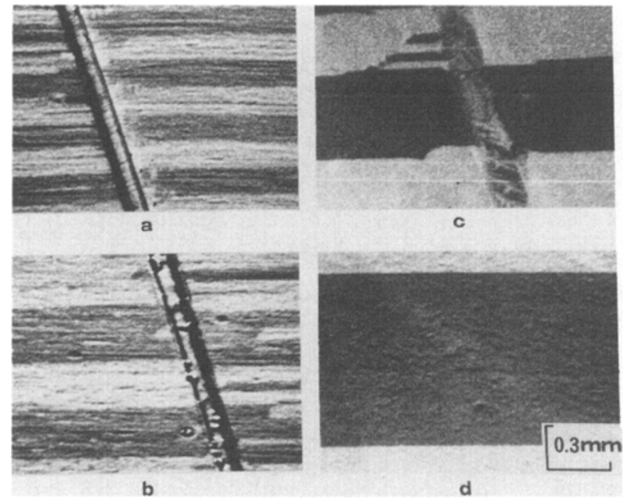

Fig. 8 (a) Domain patterns of strain-introduced, grain-oriented 3% silicon steel. (b) After removing glass film. (c) Grooves were removed by chemical polishing. (d) Annealed in hydrogen atmosphere at 1200 °C for 20 h. Courtesy of Dr. Nozawa (Ref 7)

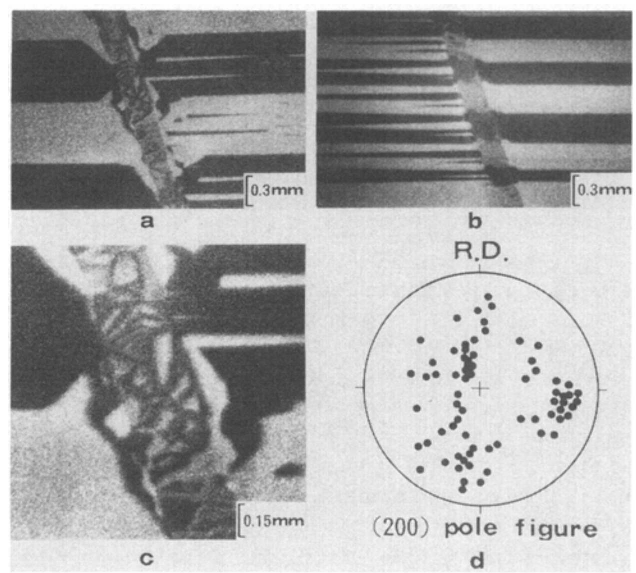

Fig. 9 (a) Domain images of small grains. (b) Crystal orientations of micrograins. Courtesy of Dr. Nozawa (Ref 7)

3.4 *Micrograin Shapes Versus Iron Loss*

Figure 7 shows the relationship between the depth of micrograins formed on a steel sheet and their magnetic properties. Each width of the tip had the optimum depth of micrograins. In the case of the 85 μm tip, the iron loss of $W_{17/50}$ was a minimum at 140-μm-deep micrograins, and of $W_{13/50}$, at more than 160-μm-deep micrograins. On the other hand, the 35 μm tip had a minimum iron loss of $W_{17/50}$ at 100-μm-deep micrograins, and of $W_{13/50}$, at 100-μm-deep micrograins. The effect of decreasing iron loss was larger in the 35 μm tip than in the 85 μm tip.

3.5 *Discussions about the Loss-Reduction Mechanism*

Magnetostatic energy is clearly a major driving force for the creation of domain refining in a grain-oriented silicon steel. The loss-reduction mechanism from the magnetostatic energy is discussed.

The magnetostatic energy can be reduced to zero by the introduction of subdomains with transverse magnetization if a specimen is not under tensile-stressed state. By applying tensile stress along the [001] direction, these subdomains disappear due to the interaction between magnetostriction and tensile stress. Simultaneously, the main domain wall spacings are refined to multidomain.

For example, Fig. 8 shows the changes of domain structure in a specimen with and without glass film, which means relieving tensile stress (Ref 7). Figure 8(a) shows the domain structure in a specimen with glass film. The 180° main domain wall spacing enlarged, and many subdomains appeared near the grooves (Fig. 8b). Subsequently, the grooves were shaved off by mechanical polishing and stress-relief annealed. A line of small grains crossed the main domain. Various types of subdo-

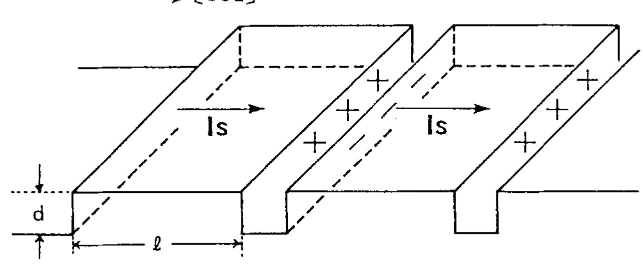

Fig. 10 Models of magnetostatic energy for grooves

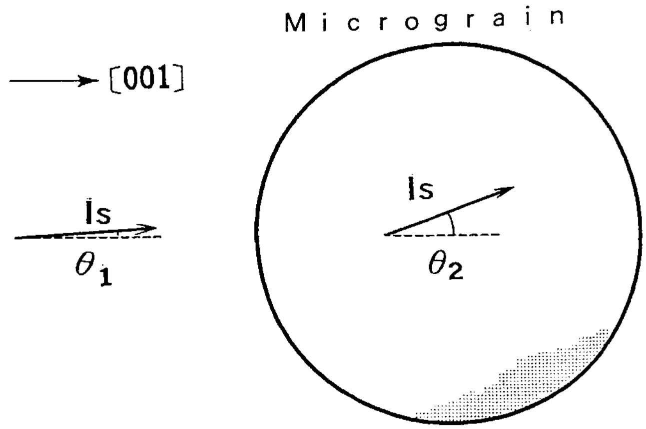

Fig. 11 Models of magnetostatic energy for micrograins

mains occurred in the vicinity of the micrograins line (Fig. 8c). After heat treatment at 1200 °C for 20 h in a hydrogen atmosphere, these small micrograins disappeared, and simultaneously the 180° main domain wall spacing enlarged (Fig. 8d).

These small grains were largely misoriented from (110)[001] (shown in Fig. 9b) (Ref 7). Existence of these micrograins contributed to the formation of subdomains with transverse magnetization and/or spikelike domains. Misorientation of micrograins from (110)[001] was random.

From these observations, the approximate effect of grooves and micrograins on magnetostatic energy was estimated. At first, the magnetostatic energy due to grooves was estimated. Figure 10 shows the models of grooves. The magnetostatic energy, E_s, of the surface rectangular area between two grooves can be expressed by:

$$E_s = \frac{1}{2} N_D \Delta I_n{}^2 \qquad \text{(Eq 1)}$$

where N_D is the demagnetizing factor and ΔI_n is the difference of the horizontal component of the magnetization vector. The N_D was considered to approximate the surface rectangular area between two grooves to oblate ellipsoid (Ref 11). For example, if the depth of the groove is 25 μm and the spacing of grooves is l = 5000 μm, N_D is about 0.05. The ΔI_n is nearly equal to a magnetization of 3% Si-Fe 1630 gauss (I_s). The magnetostatic energy, E_s, of groove is about 0.7×10^5 erg/cc. If the depth of grooves is bigger than 25 μm, N_D will be larger. The magnetostatic energy, E_s, also will be larger.

Next, the magnetostatic energy due to micrograins was calculated. Figure 11 shows the models of micrograins. Grain boundaries in a polycrystalline specimen separate regions of different crystallographic orientation or easy-magnetization direction. Consequently, there is generally a discontinuity across the boundaries in the magnetization-vector component normal to the boundary. Therefore, magnetic poles exist at the grain boundaries, and the magnetostatic energy is associated with these poles. The magnetostatic energy, E_s, of micrograins can be expressed by Eq 1. The grain-boundary surface pole density, ΔI_n, can be expressed by (Ref 12):

$$\Delta I_n = I_s (\cos \theta_1 - \cos \theta_2) \qquad \text{(Eq 2)}$$

From the observation in Fig. 9, $\theta_1 = 0°$ and $\theta_2 = 15°$. If the shape of micrograins can be approximated to the sphere, N_D is 4/3 π. The magnetostatic energy, E_s, of the sphere is 0.07×10^5 erg/cc. From these calculations, the potentiality of micrograins for the domain refining is about one tenth that of grooves.

4. Conclusions

To clarify the effect of various shapes of grooves and micrograins on magnetic properties, many types of microstructure of heatproof, domain-refined, grain-oriented silicon steel sheets were investigated.

The micrograins were generated from the surface of grove and grew at 45° angles from the surface of the sheet, which is the area with the highest level of hardness. The effect of decreasing the iron loss value was larger in narrow and deep grooves than in wide and shallow grooves.

From the calculations of the magnetostatic energy, the potentiality of micrograins for the domain refining is about one tenth that of grooves.

Acknowledgments

The authors thank Dr. T. Nozawa, Department of Electrical Engineering, Kyushu Kyoritsu University, for his helpful advice and discussions of this paper. And they also thank H. Honma and Y. Matsuo, Yawata R&D Laboratories, Nippon Steel Corp., for their helpful contributions to this work.

References

1. K. Kuroki, K. Fukawa, and T. Wada, *J. Appl. Phys.*, Vol 52, 1981, p 2442
2. P. Beckely, D. Snell, and C. Lockhart, *J. Appl. Phys.*, Vol 57, 1985, p 4212
3. T. Iuchi, S. Yamaguchi, T. Ichikawa, N. Nakamura, T. Ishimoto, and K. Kuroki, *J. Appl. Phys.*, Vol 53, 1982, p 2410
4. M. Nakamura, K. Hirose, T. Iuchi, S. Yamaguchi, and Y. Ohya, *IEEE Trans. on Mag.*, Mag-18, 1982, p 1508
5. J.W. Shoen and A.L. Von Holle, The 1986 ASM Materials Week Conference, American Society for Metals, 1986
6. M. Yabumoto, H. Kobayashi, T. Nozawa, K. Hirose, and N. Takahashi, *IEEE Trans. on Mag.*, Mag-23, 1987, p 3062

7. T. Nozawa, Y. Matsuo, O. Tanaka, H. Kobayashi, and K. Kuroki, ASM International Proceeding, report No. 8710-003, ASM International, 1987
8. H. Kobayashi, K. Kuroki, E. Sasaki, M. Iwasaki, and N. Takahashi, *Soft Magnetic Materials Conf. Digests 4.02*, 1987
9. H. Kobayashi, K. Kuroki, E. Sasaki, M. Iwasaki, and N. Takahashi, *Phys. Scr.*, Vol T24, 1988, p 36-41
10. K. Fukawa and T. Yamamoto, *IEEE Trans. on Mag.*, Mag-18, 1982, p 963
11. R.M. Bozorth, *Ferromagnetism*, D. Van Nostrand Company, Inc., p 849
12. J.B. Goodenough, *Phys. Rev.*, Vol 95, 1954, p 917